Research Article

SURFACE and INTERFACE ANALYSIS

Received: 18 August 2007 Revised: 15 November 2007 Accepted: 19 November 2007 Published online in Wiley Interscience: 8 January 2008

(www.interscience.com) DOI 10.1002/sia.2722

ToF-SIMS study of 1-dodecanethiol adsorption on Au, Ag, Cu and Pt surfaces

Taina Laiho* and Jarkko A. Leiro

Time-of-flight secondary ion mass spectrometry (ToF-SIMS) has been used to perform a chemical analysis of long-chain thiol ($CH_3(CH_2)_{11}SH$)-treated gold, silver, copper and platinum surfaces. All the mass peaks from positive and negative ion spectra within the range $m/z = 0-2000$ u are studied. ToF-SIMS data revealed that on gold, silver and copper substrates 1-dodecanethiol form dense standing-up phases, but on platinum being a catalytically active substrate, we were able to identify also surface-aligned parallel lying molecules in addition to a standing thiolate layer. Our study shows that when ToF-SIMS spectra are analyzed, not only the existence of oligomers but also metal + hydrocarbon fragments give information about the order of SAM. Copyright © 2008 John Wiley & Sons, Ltd.

Keywords: self-assembled monolayers; time-of-flight secondary ion mass spectrometry; *n*-dodecanethiol; adsorption; surfaces

Introduction

Self-assembled monolayers (SAMs) are spontaneously formed, well ordered, one-molecule-thin films on surfaces. They can be obtained using different types of molecules and substrates. We have used a thiol (1-Dodecanethiol, $CH_3(CH_2)_{11}SH$) solution to create uniform SAMs on metals. The molecules utilized in self-assembly processes consist of a surface-active headgroup having a bonding to the substrate by chemisorption, and a molecular body, which is standing away from the surface. The ability to tailor both the head and tail groups of the constituent molecules makes these thin organic films useful having both theoretical and technological importance. The SAMs control interactions on the metal/environment interface. They can be useful in many kinds of applications:[1] for instance, in biology,[2–4] controlling wetting properties,[5] lithographical applications,[6,7] molecular electronics, and sensors.[4,8–10] They also protect metals against corrosion.[11,12]

SAMs have been intensively investigated over the past decades. An accurate determination of the composition, quality, and coverage of SAMs is in progress.[13–15] Despite intense studies of SAMs the precise character of the sulfur/metal interaction and organization of molecules on surfaces remains unresolved in many cases.

The first mass spectrometric investigations of SAMs have been published about 13 years ago by Li *et al*.[16] Tarlov *et al*.[17] and Frisbie *et al*.[18] We have used Time-of-flight secondary ion mass spectrometry (ToF-SIMS), which has been a powerful method for analyzing monolayer surfaces.[19–24] It is a rather sensitive surface analysis technique providing information on the chemical composition and molecular structure of SAMs.[25] Recently, SAM surfaces on gold and on silver have been studied.[21–23] To our knowledge, no ToF-SIMS studies of $CH_3(CH_2)_{11}SH$ on Cu or Pt have been considered so far. In this study, we investigate ToF-SIMS data of 1-dodecanethiol adsorbed on Au, Ag, Cu and Pt surfaces. Comparing different metals that are treated the same way, gives information about the significance of a substrate to the layer formation. One purpose of the now-presented study is to extend our earlier analysis,[26] where we suggest a dialkyl sulfide formation on the platinum surface during the dodecanethiol adsorption process.

Experimental

Sample preparation

The SAMs were prepared on polycrystalline gold, platinum, silver (all from Goodfellow), and copper (Outokumpu Copper, Finland) substrates by a spontaneous adsorption from the solution. Prior to the adsorption, the surface (area *ca* 0.5 cm^2) was wet-polished with a SiC grinding paper (1000 and 4000 mesh) and washed with pure water. The sample was then transferred to the treatment solution. Dodecanethiol, $CH_3(CH_2)_{11}SH$ (marked $C_{12}SH$ or M later in the text), was used for a chemical treatment of the specimen. Thiol was utilized as purchased from Aldrich (99%). Surfaces were immersed in a 1 mM solution of thiol in deoxygenated ethanol for approximately 24 h. After this treatment, every sample was carefully rinsed with ethanol and water to remove the weakly adsorbed species.

Film characterization

The ToF-SIMS spectra were measured with a ToF-SIMS PHI TRIFT II (Physical Electronics Inc., Eden Prairie, USA). The instrument was equipped with a liquid metal $^{69}Ga^+$ primary ion gun and a high mass-resolution time-of-flight mass analyzer.

Thin organic layers are very sensitive to the ion beam damage. The situation has been taken into account by performing all the ToF-SIMS measurements under static conditions. Positive and negative ion mass spectra were detected from an area of $200 \times 200\ \mu m^2$. Total ion doses of 4.7×10^{11} ions/cm^2 were used to acquire spectra. The WinCadence program was used for the

* *Correspondence to: Taina Laiho, Laboratory of Materials Science, University of Turku, FIN-20014 Turku, Finland. E-mail: taina.laiho@utu.fi*

Laboratory of Materials Science, University of Turku, FIN-20014 Turku, Finland

analysis of measured mass spectra. The peak assignments have been made on the basis of the exact mass value and the isotopic distribution of atoms.

Results

Secondary ions were obtained over a mass range of 0–2000 a.m.u. Characteristic peaks associated with the thiolate molecules appear in the mass spectra. As can be suspected, a combination of organic, metal-organic and metal clusters are observed.

Metal ions

In all measurements, substrate signals were also found. In the positive ion spectra, the following components attributed to metal atoms and clusters can be seen: Au^+ at $m/z = 197$, Au_2H^+ ($m/z = 395$), Au_3^+ ($m/z = 591$), Au_4H^+ ($m/z = 789$), Au_5^+ ($m/z = 985$), Au_6H^+ ($m/z = 1183$) and Au_7^+ ($m/z = 1379$); Ag^+ ($m/z = 107$ and 109), Ag_2^+ ($m/z = 214$, 216 and 218) Ag_3^+ ($m/z = 321$, 323, 325, and 327), Ag_4^+ ($m/z = 428–436$), Ag_5^+ ($m/z = 534–545$); Cu^+ ($m/z = 63$ and 65), Cu_2^+ ($m/z = 126$, 128 and 130), Cu_3^+ ($m/z = 189$, 191, 193, and 195); Pt^+ ($m/z = 192$, 194, 195, 196, and 198) and Pt_2^+ ($m/z = 384–396$). Positive ToF-SIMS spectra associated with metal and metal clusters are presented in Figs 1–4. Number of detected isotopes and their relative intensity can be seen in the spectra. Metal and metal cluster peaks are also present in the negative ion spectra. These ions originate from the substrate that is buried by the organic layer.

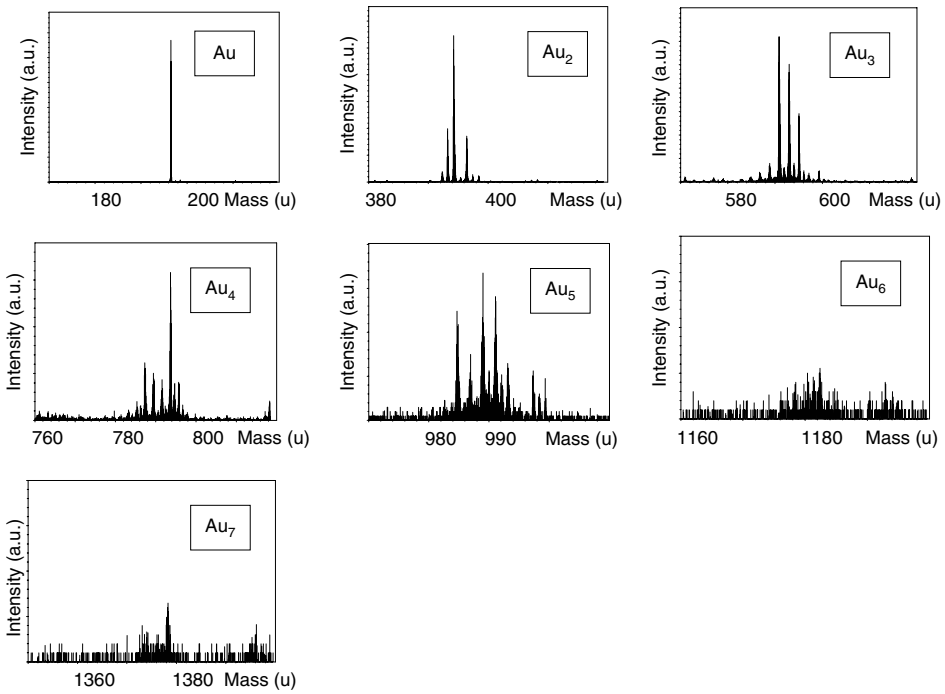

Figure 1. Positive ToF-SIMS spectra of $C_{12}SH$ treated Au. Peaks associated with gold and the corresponding metal clusters are presented.

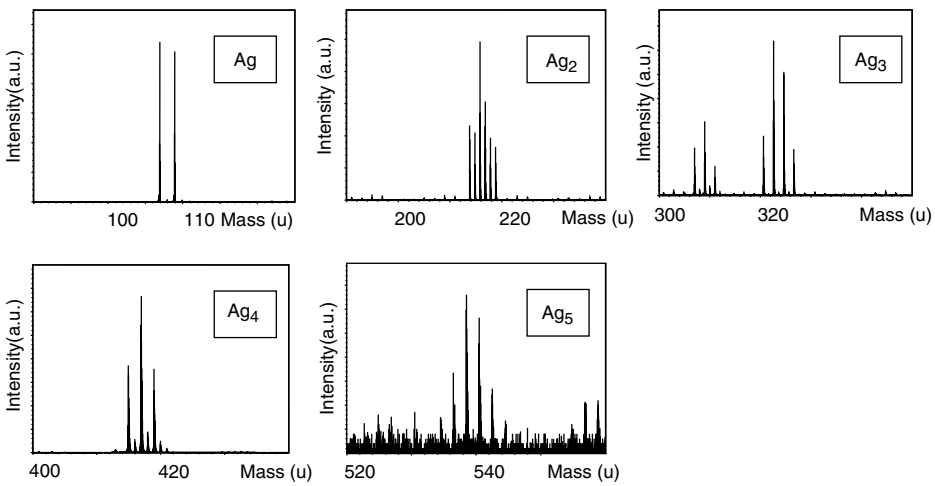

Figure 2. Positive ToF-SIMS spectra of $C_{12}SH$-treated Ag. Peaks associated with silver revealing two isotopes and the corresponding metal clusters are presented.

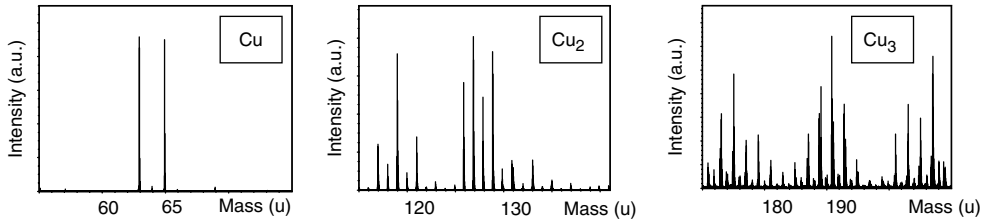

Figure 3. Positive ToF-SIMS spectra of $C_{12}SH$-treated Cu. Peaks associated with copper (two isotopes) and the corresponding metal clusters are presented.

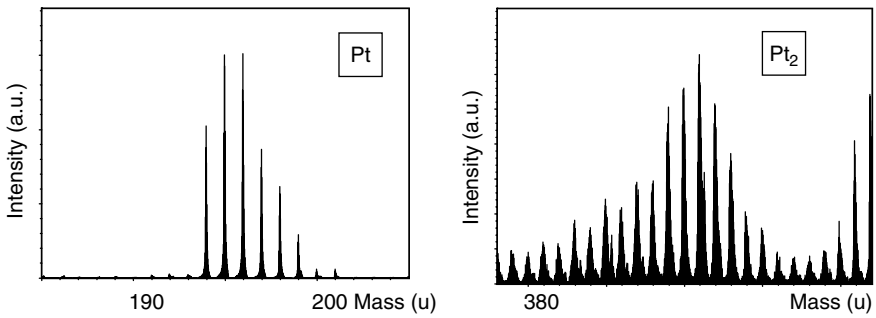

Figure 4. Positive ToF-SIMS spectra of $C_{12}SH$-treated Pt. Peaks associated with platinum atoms giving six clear isotopes, and the corresponding metal clusters are presented.

Hydrocarbon fragments

Positive secondary ion emission spectra are dominated by a pattern characteristic of long-chain hydrocarbons, namely $C_xH_y^+$. Most of these fragments can be assumed to originate from the hydrocarbon chains of thiol molecules. The mass region $m/z = 0–60$ for all the studied substrate materials is presented in Fig. 5. Small methyl ion CH_3^+ peak at $m/z = 15$ can be seen in the presented spectra. The most abundant species at $m/z = 27$, 29, 41, 43, 55, and 57 are obtained from $C_2H_3^+$, $C_2H_5^+$, $C_3H_5^+$, $C_3H_7^+$, $C_4H_7^+$, and $C_4H_9^+$, respectively. These peaks originating from alkyl chain fragments are accompanied with other peaks where one or more carbon–carbon double bonds are formed under removal of one or more hydrogen atoms during the sputtering process.

The low-mass region ($m/z = 0–50$) of negative ion spectra exhibits a small fragment sequence, which is quite similar for all the studied samples. In Fig. 6 the principal features in the low-mass region of negative SIMS are shown. They arise from CH^- ($m/z = 13$), C_2H^- ($m/z = 25$), S^- ($m/z = 32$), and SH^- ($m/z = 33$) species. Also, O^- and OH^- peaks can be seen in the spectra ($m/z = 16$ and $m/z = 17$, respectively). This part of the spectra consisting of peaks attributed to small ions that result from chain fragmentation of used thiol molecules does not seem to provide information about the molecular ordering but only about the chemical concentration of the surface.

Even though the ToF-SIMS is a chemical surface analysis technique, it also can give information on the SAMs order. In the spectra measured from $C_{12}S$/Pt, sample platinum peaks (Pt^+, Pt_2^+ ...) are accompanied with those associated to metal + hydrocarbon clusters, whereas the spectra measured from $C_{12}S$/Au, $C_{12}S$/Ag, and $C_{12}S$/Cu reveal no prominent mass peaks on the higher-mass side of the metal peaks, being consistent with the fragments of hydrocarbon chains. The situation can be seen in Fig. 7. Indeed, this is the result concerning the order of the SAM. Metal + hydrocarbon fragments observed at the $C_{12}S$/Pt specimen are supposed to originate from lying thiols that exist on the surface.

Sulfur-containing species

Several peaks corresponding to sulfur-containing clusters are observed. Ranges from 150 to 700 a.m.u. are presented in Fig. 8. All the sulfur can be assumed to be brought to the surface by thiol molecules, though its existence assures the adsorption. Both S^- and SH^- fragments are present on all the studied surfaces at $m/z = 32$ and 33, respectively. The existence of molecular ion clusters emitted from the surface ($[M-H]^{-,+}$, $[MeM-H]^{-,+}$, $Me_2[M-H]^{-,+}$, and $Me[M-H]_2^{-,+}$, where $M = CH_3(CH_2)_{11}SH$ and Me = Au, Ag, Cu, or Pt) is detected. Also, clusters consisting of metal + sulfur are detected in every spectra, since the surface layer absorbs energy from collisions, and that results in breaking of the C–S bond of the molecules.[27]

Molecular fragments containing sulfur and parts of hydrocarbon chain (RS^-) are detected. The existence of molecular ion clusters emitted from the surface is an evidence of the formation of a thiolate layer. Large clusters like $Me_2[M-H]_3^-$ and $Me_3[M-H]_4^-$ can be seen in the studied negative ion spectra in case the bulk metal is Au, Ag, or Cu, but only very small peaks originating from large molecular clusters are seen in the platinum specimen.

In the negative ion spectrum of a $C_{12}S$/Au sample, the most intense molecular ion peak that is observed is $Au[M-H]_2^-$ ($m/z = 599$) in Fig. 8. The formation of the $Au[M-H]_2^-$ species is not supposed to be a result only from the intact ejection but also from a recombination reaction that occurs somewhere above the surface during the secondary ion emission process.[21] It can also result in an emission from defect sites such as those that might be encountered at Au steps or grain boundaries.[17] Moreover, sizes of the peaks originating from $Au_2[M-H]^-$ ($m/z = 595$) and from $Au[M-H]^-$ ($m/z = 399$) are remarkable, but the signal associated with deprotonated thiol $[M-H]^-$ ($m/z = 201$) is very small. One factor, that may contribute to the high probability of an ejection of intact Au + molecular thiol clusters and the small size of the peak connected to the deprotonated thiol, is the stability of the Au–S bond where the heat of adsorption of about 30 kcal/mol has been measured for thiolates on Au.[17,28] Also, bigger cluster ions $Au_2[M-H]_3^-$ ($m/z = 997$) and even $Au_3[M-H]_4^-$ ($m/z = 1395$)

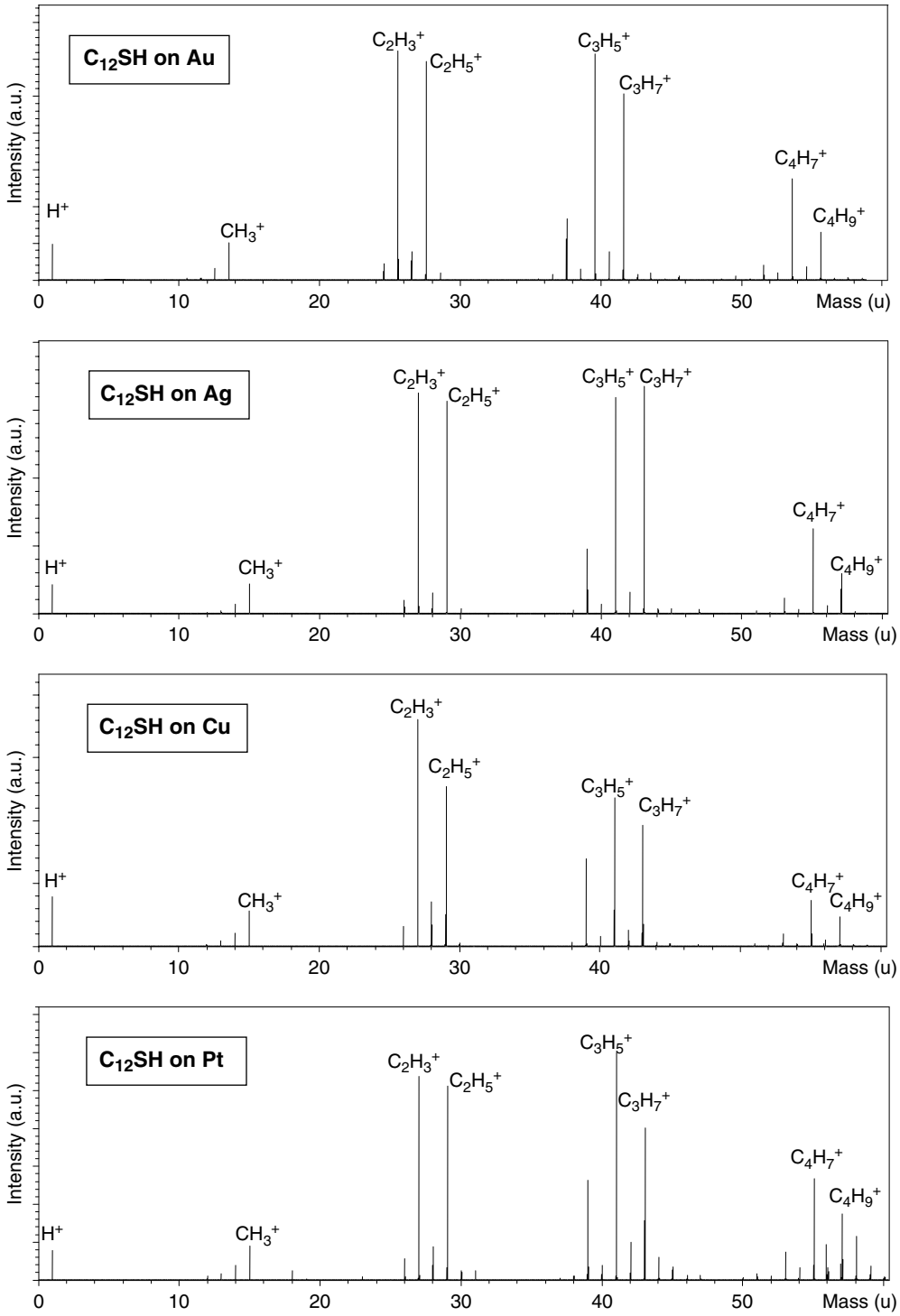

Figure 5. Positive ToF-SIMS spectra of $C_{12}SH$-treated Au, Ag, Cu, and Pt surfaces. Positive secondary ion emission spectra are dominated by a fragment pattern characteristic of long-chain hydrocarbons, namely, $C_xH_y^+$. Most of these fragments can be assumed to originate from the hydrocarbon chains of thiol molecules.

are clearly visible in the spectrum (not shown). Due to the strong Au–S bond at the metal thiol interface, various gold–sulfur cluster ions such as AuS^-, (m/z = 229) Au_2S^- (m/z = 426), $Au_2S_2H^-$ (m/z = 459), Au_3S^- (m/z = 623), $Au_3S_2^-$ (m/z = 655,) and $Au_3S_3^-$ (m/z = 687) are found. On positive ion spectra the intensities of various gold and gold–sulfur cluster ion peaks exceed those of molecular secondary ion ones.

On the silver substrate, a significant peak in the negative ion spectrum is present at m/z = 201 corresponding to the $[M-H]^-$ ions. The observed peak of $Ag[M-H]^-$ (m/z = 309 and 311) is barely visible but the signal of $Ag[M-H]_2^-$ (m/z = 509 and 511) is big (Fig. 8). The peaks of $Ag_2[M-H]^-$ (m/z = 415, 417, and 419), $Ag_2[M-H]_3^-$ (m/z = 817, 819, and 821) and $Ag_3[M-H]_4^-$ (m/z = 1125–1131) are also visible (Fig. 9). The

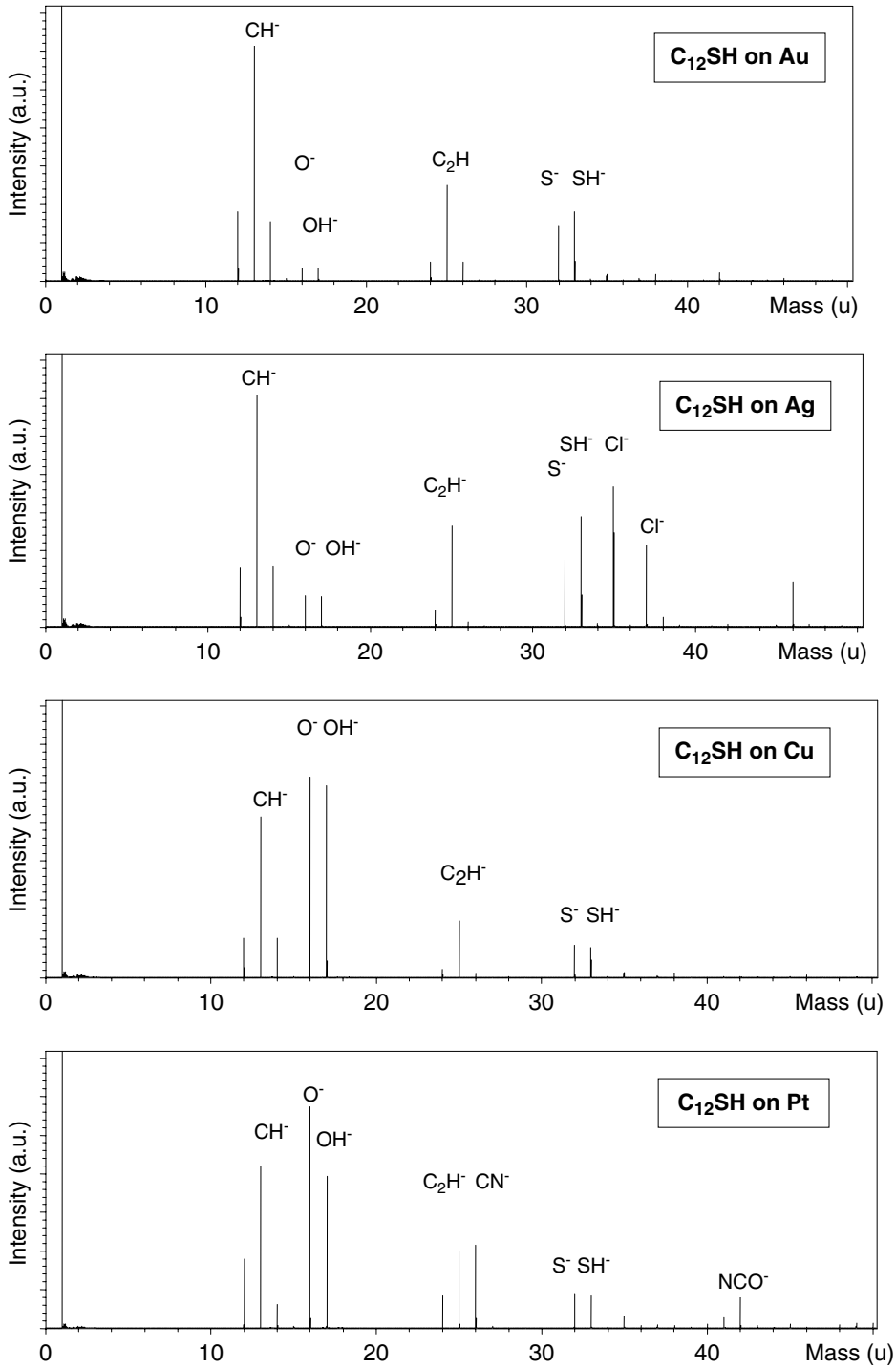

Figure 6. Negative ToF-SIMS spectra of $C_{12}SH$-treated Au, Ag, Cu, and Pt surfaces for lower-mass fragments. This part of the spectra consists of peaks attributed to small ions that result from the chain fragmentation. It provides information about the chemical concentration of the surface.

relative intensity of the $[M - H]^-$ peak is more pronounced than that of the spectra measured from the thiol-treated Au, which is surprising since the strength of the thiolate-substrate bond for silver is even stronger than that for gold. The Ag–S bond is expected to be more ionic than the Au–S bond based on the electronegativity differences between S and these two metals.[29] The strength of the S–Ag bond is supposed to result in a weaker S–C bond of the alkyl chain for the latter system and to decrease the amount of releasing $[M - H]^-$ ions.[30] The peaks associated with Ag_2SH^+ (m/z = 247, 249, 251, and 253), $(Ag_2S)_2H^+$ (m/z = 493–501), Ag_3S^+ (m/z = 353, 355, 357, and 359), Ag_4SH^+ (m/z = 461–471), Ag_5S^+ (m/z = 566–576) are all detectable (Fig. 10). Secondary ions of the form $[M - H + Ag]^+$ are common in SIMS studies of LB films on Ag, which is not the case when substrate material is Au, Cu, or Pt.[18] Indeed, several thiolate + silver clusters are present in the positive ion spectra.

On the copper surface, the $[M - H]^-$ peak (m/z = 201) is stronger than those of $Cu[M - H]^-$ (m/z = 265, 267),

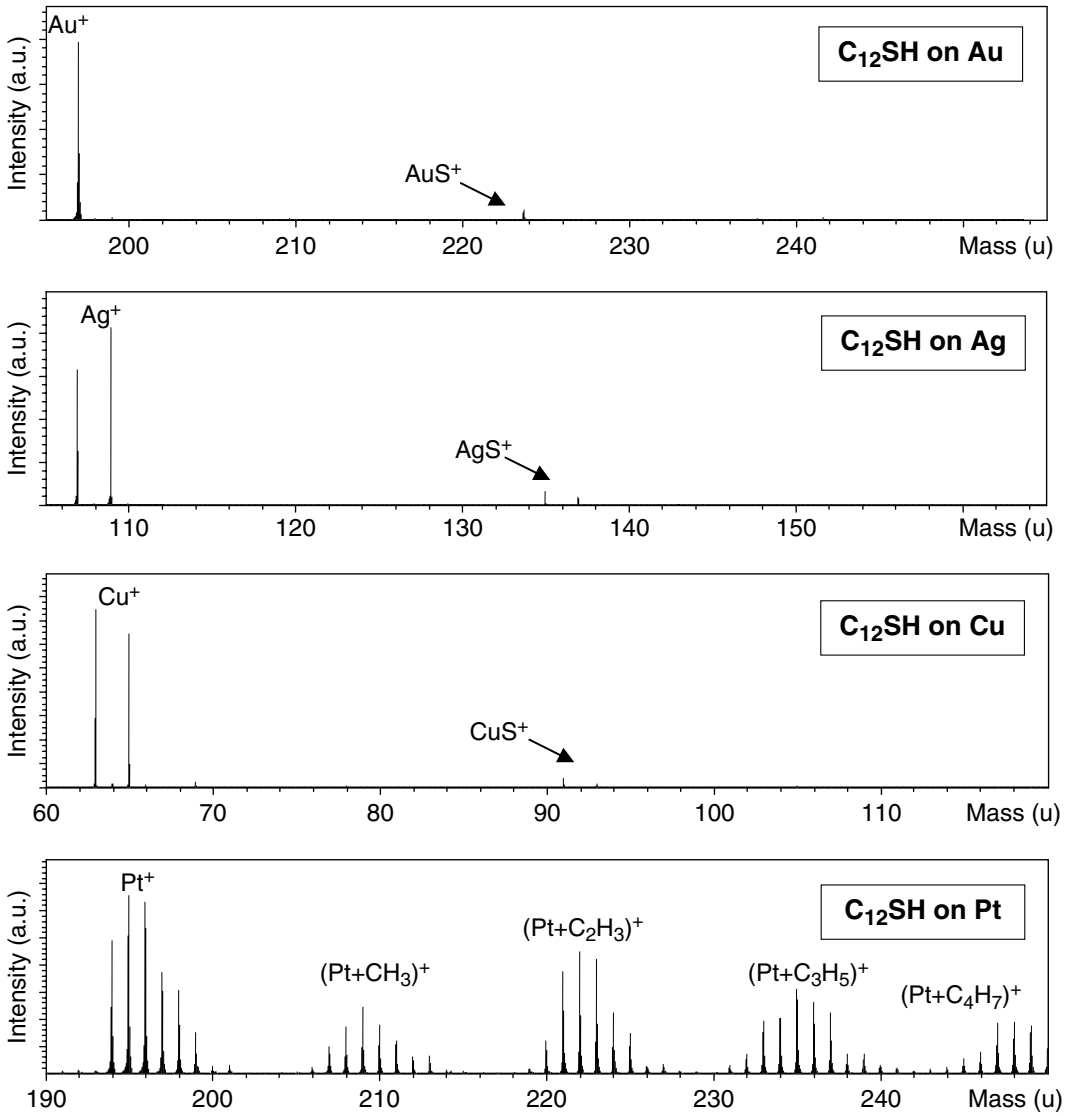

Figure 7. Positive ToF-SIMS spectra of $C_{12}SH$-treated Au, Ag, Cu, and Pt surfaces. On the left hand side of each 60 a.m.u.-wide spectrum window are metal ion peaks and on the higher m/z on the right hand side are metal + sulfur ($m/z = 32$) lines and those connected to metal + fragments of hydrocarbon chains. In the spectra measured from $C_{12}S$/Pt, sample platinum peaks (Pt^+, $Pt_2{}^+$ ...) are accompanied with those associated with metal + hydrocarbon clusters, whereas the spectra measured from other substrates reveal no such components.

$Cu[M-H]_2{}^-$ ($m/z = 465, 467$), $Cu_2[M-H]_3{}^-$ ($m/z = 729, 731, 733$) or $Cu_3[M-H]_4{}^-$ ($m/z = 993-999$) (Fig. 11). Some copper sulfides CuS ($m/z = 95, 97$) or Cu_2S ($m/z = 158, 160, 162$) are also detected in the case of the positive ion spectrum. The Cu–S interaction is strong. For ethanethiolate adsorbed on Cu(100) binding energies between 55–72 kcal/mol have been calculated.[31] Previous studies have shown that heating the copper thiolate films above room temperature causes a S–C bond breaking and a desorption of the entire alkyl chain.[32] Since this kind of dissociative desorption is typical for copper thiolate films, our ToF-SIMS spectra show only small or moderate size molecular ion peaks, and in addition to them, features attributable to copper + molecular ion fragments are seen. In addition, strong peaks can be observed for fragments of hydrocarbon chains, and also for copper clusters, and for copper sulfide species.

In the case of the platinum substrate, Pt + hydrocarbon clusters dominate in the spectra. Only $Pt[M-H]_2{}^-$ ($m/z = 596-600$) from possible molecular ion clusters can be undoubtedly detected in the spectrum (Fig. 12). No Pt_xS_y species are observed even if Pt–S binding energy has been calculated to be strong (56 kcal/mol).[33]

Oxygen

In the negative ion mode, oxygen peaks (O^- and OH^-, at $m/z = 16$ and 17) are present in the spectra measured from Cu and from Pt samples. Oxidized hydrocarbon fragments (with no sulfur atoms present) were not observed. The XPS spectra of $C_{12}S$/Cu typically show the presence of some oxygen-containing species on the surface. The possible existence of several copper oxide cluster ions has been checked. Some Cu_2O was detected on the surface, but CuO, CuOH, and $Cu(OH)_2$ were not found. On the platinum substrate, more oxygen-containing species were seen than in the corresponding spectra from the other substrate materials. Sulfonates are formed by air oxidation of SAMs.[29,34] The $SO_3{}^-$ ($m/z = 80$) and $HSO_4{}^-$ ($m/z = 97$), are found on all the

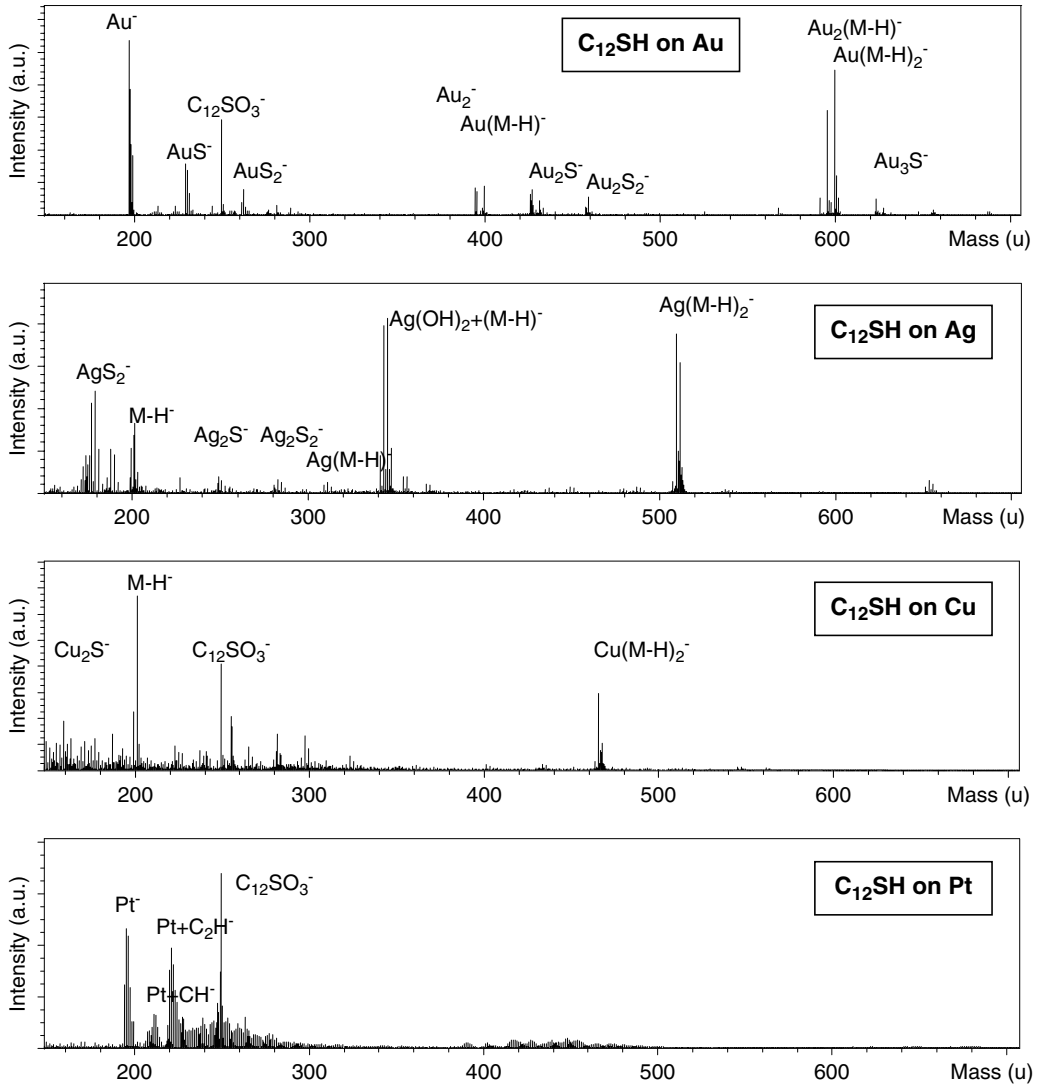

Figure 8. Negative ToF-SIMS spectra of $C_{12}SH$-treated Au, Ag, Cu, and Pt surfaces in the case of large clusters. Peaks corresponding to sulfur-containing clusters are observed. All the sulfur contribution can be assumed to be brought to the surface by thiol molecules, though its existence assures the adsorption.

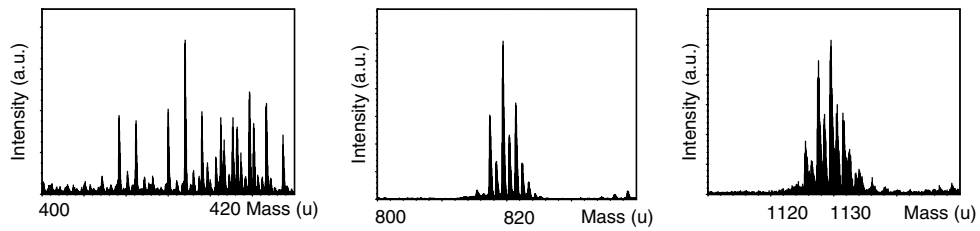

Figure 9. Negative ToF-SIMS spectra of $C_{12}SH$-treated Ag surface. Large molecular ion clusters are presented. The peaks of $Ag_2[M-H]^-$ (m/z = 415, 417, and 419), $Ag_2[M-H]_3^-$ (m/z = 817, 819, and 821) and $Ag_3[M-H]_4^-$ (m/z = 1125–1131) are shown.

studied surfaces. The amount of sulfonate ions (SO_3^- and HSO_4^-) compared to the metal ions (Au^-, Ag^-, Cu^-, or Pt^-) is presented in the Table 1. Also, $CH_3(CH_2)_{11}SO_3^-$ (m/z = 249) is seen in the negative ion spectra of Au, Cu, and Pt (Fig. 8).

Other species

A chlorine contamination can be seen in the Ag spectrum (Fig. 6), but not in the other spectra. Chlorine is a common impurity and it can originate, e.g. from water or short atmospheric exposure between solution treatment and ToF-SIMS analysis.[17,22] Silver forms more insoluble salts than any other metal, and it may have formed an AgCl compound during the sample preparation.

Nitrogen species (CN^- and NCO^-) are present on the platinum substrate where the thiolates have not only formed just a perfectly organized standing thiolate layer, but also areas with lying chains and dialkylsulfide species. The presence of nitrogen impurities can

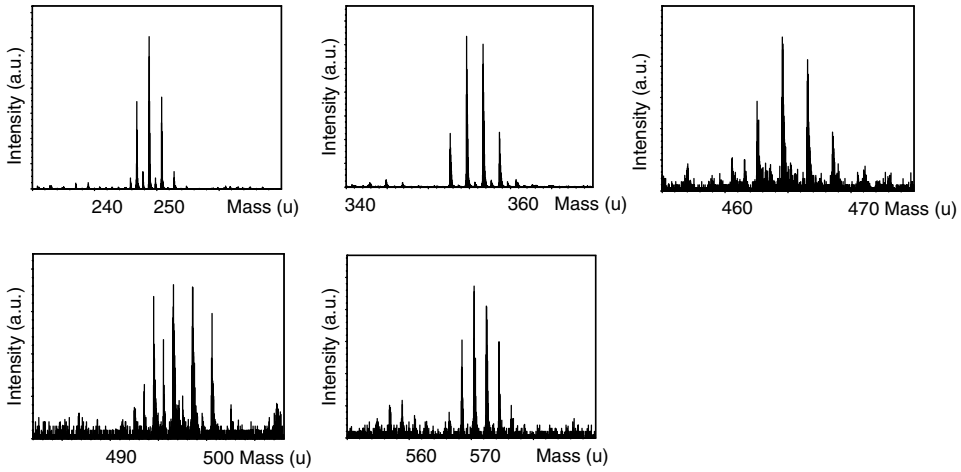

Figure 10. Positive ToF-SIMS spectra of $C_{12}SH$-treated Ag surface. Peaks associated to large sulfur-containing clusters are described. The peaks associated with Ag_2SH^+ (m/z = 247, 249, 251, and 253), Ag_3S^+ (m/z = 353, 355, 357, and 359), Ag_4SH^+ (m/z = 461–471), $(Ag_2S)_2H^+$ (m/z = 493–501) and Ag_5S^+ (m/z = 566–576) are observed.

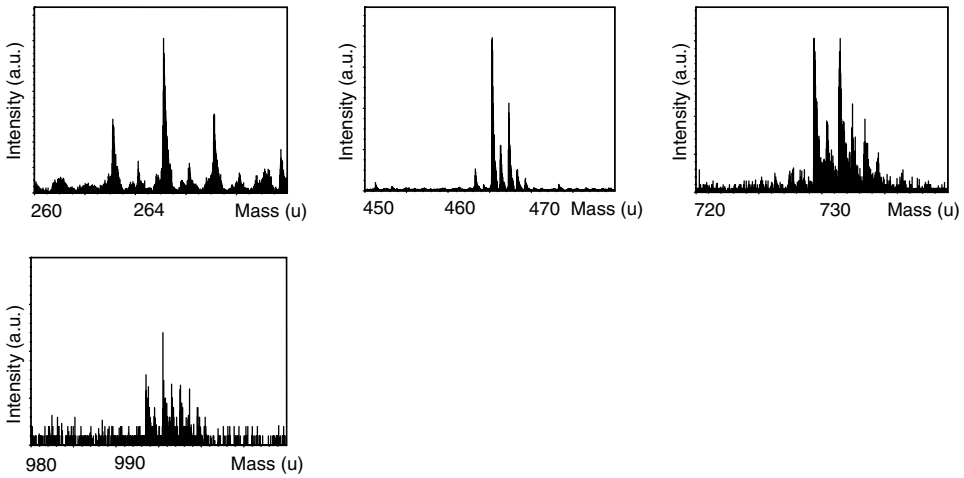

Figure 11. Negative ToF-SIMS spectra of $C_{12}SH$-treated Cu surface. Large molecular ion clusters are obtained. The peaks associated with CuM^- (m/z = 265, 267), $Cu[M-H]_2^-$ (m/z = 465, 467), $Cu_2[M-H]_3^-$ (m/z = 729, 731, 733) and $Cu_3[M-H]_4^-$ (m/z = 993–999) are shown.

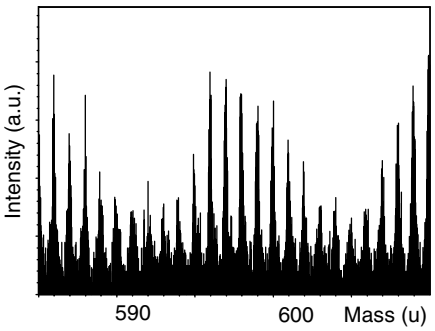

Figure 12. Negative ToF-SIMS spectra of $C_{12}SH$-treated Pt surface. Peaks associated with $Pt[M-H]_2^-$ are presented. The large number of components in the mass spectra of platinum is due to the existing platinum isotopes.

Table 1. The relative concentration of observed metal and sulfonate species. The relative intensity of detected metal ions (Me^-) is normalized to 100 a.u

	Intensity (a.u.)			
Fragment	Au	Ag	Cu	Pt
Me^-	100	100	100	100
SO_3^-	18	24	13	62
HSO_4^-	13	27	13	37

be a consequence of the catalytic activity of platinum breaking of some of the hydrocarbon chains. The CN^- ion has a triple bond that has a high bonding energy and will not break easily during the sputtering, and the CN radical has a high electron affinity of 3.82 eV and accepts a negative charge easily.[35,36] That is why it is detected with high sensitivity by ToF-SIMS.

Discussion

Substrate signal was detected from Au, Ag, Cu, and Pt in spite of the thiolate layer on top of the samples. Also, sulfur can be identified in the measured spectra. Presence of sulfur on the surfaces is a

consequence of thiol treatment. The existence of the fragments of hydrocarbon chain ($C_xH_y^+$) is very obvious for all of the studied samples, and it ensures that the surface is covered with an organic layer. Long hydrocarbon chains of the surface thiolates are tightly held together via secondary forces such as hydrophobic and van der Waals interactions. These interaction energies can make it more difficult for longer hydrocarbon chains to be emitted from the SAM surface. That is why fragments of very long chains are not detected.

Intense peaks associated with platinum + short hydrocarbon fragments are observed. Assuming that the thiol chains are lying parallel to the surface or are arranged as a loosely organized submonolayer, the hydrocarbon chains are more accessible to random fragmentation by the incoming ions. This results in a range of short and midsize fragments from the hydrocarbon backbone and peaks due to metal+hydrocarbon fragments. This observation is consistent with our earlier report (Ref. [26]) suggesting that due to the catalytic activity of platinum, the substrate interacts with molecules lying parallel to the surface during the first step of the adsorption. Then the fragmentation of carbon chains may take place. Platinum partially dehydrogenates the adsorbed chains forming hydrocarbon radicals and adsorbed alkenes, and this can be seen in the now-presented ToF-SIMS spectra.

The ion yields of oligomers, made of several alkanethiol chains bound to metal atoms, provide a method to measure the overlayer order, or the self-assembly. The necessary conditions to emit such ions are a high surface coverage and a dense packing of the SAM.[23] Many molecular clusters are identified from the gold, silver, and copper substrate, and some from the platinum substrate. The observation of longer fragments and molecular ions, also in the case of the platinum sample, is in line with the assumption of the earlier published XPS data[26], in the sense that also the organized thiolate phases are formed on the platinum surface.

It is a known fact that controlled photo-oxidation converts the thiolate to sulfonate species.[29] The SO_3^- and HSO_4^- are observed on all the studied surfaces. $CH_3(CH_2)_{11}SO_3^-$ is detected in the negative ion spectra of Au, Cu and Pt. It is possible that a very small fraction of the SAM has been oxidized quickly, prior to the sample insertion to the mass spectrometry. The sulfur from the thiol would also be more accessible to oxidation if the structure of thiolate layer is loosely arranged, or only partly arranged, as we suppose is the case with the platinum substrate. Indeed, the relative amount of sulfonate species compared to metal ions is bigger on platinum surface than on the other studied surfaces.

Conclusions

In conclusion, ToF-SIMS have been measured for a series of samples. SAMs prepared from 1-dodecanethiol on gold, silver, copper, and platinum samples can be successfully characterized using ToF-SIMS. The detected spectra show a rich variety of molecular secondary ions. The negative and positive ion spectra display peaks due to typical fragmentations of hydrocarbon chains and peaks connectable to the molecular ion fragments and clusters combined with metal atoms. The ToF-SIMS analysis shows that 1-dodecanethiol forms well-ordered monolayers on gold, silver and copper surfaces. The experimental data revealed also that a monolayer on platinum is not so well ordered as that on the other studied metals. According to our now-presented data, it seems that some of the molecules are lying parallel to the surface of this substrate. It is probable that the catalytic activity of platinum has affected the layer formation in the first stage of adsorption process, and some parts of the sample are covered with hydrocarbons instead of a standing tightly-packed thiolate layer.

Acknowledgements

Jyrki Juhanoja from the Top Analytica Research Company is acknowledged for his help with the ToF-SIMS measurements.

References

[1] Witt D, Klajn R, Barski P, Grzybowski BA. *Curr. Org. Chem.* 2004; **8**: 1763.
[2] Nakano K, Yoshitake T, Yamashita Y, Bowden EF. *Langmuir* 2007; **23**: 6270.
[3] Zangmeister RA, Maslar JE, Opdahl A, Tarlov MJ. *Langmuir* 2007; **23**: 6252.
[4] Dong S, Li J. *Bioelectrochem. Bioenerg.* 1997; **42**: 7.
[5] Ulman A. *Thin Solid Films* 1996; **273**: 48.
[6] Williams JA, Gorman CB. *Langmuir* 2007; **23**: 3103.
[7] Black AJ, Nealey PF, Thywissen JH, Deshpande M, El-Zein N, Maracas GN, Prentiss M, Whitesides GM. *Sens. Actuators, A* 2000; **86**: 96.
[8] Rosink JJWM, Blauw MA, Geerligs LJ, van der Drift E, Rousseeuw BAC, Radelaar S. *Mater. Sci. Eng., C* 1999; **8–9**: 267.
[9] Chaki NK, Vijayamohanan K. *Biosens. Bioelectron.* 2002; **17**: 1.
[10] Whelan CM, Ghijsen J, Pireaux J-J, Maex K. *Thin Solid Films* 2004; **464–465**: 388.
[11] Azzaroni O, Cipollone M, Vela ME, Salvarezza RC. *Langmuir* 2001; **17**: 1483.
[12] Scherer J, Vogt MR, Magnussen OM, Behm RJ. *Langmuir* 1997; **13**: 7045.
[13] Laredo T, Leitch J, Chen M, Burgess IJ, Dutcher JR, Lipkowski J. *Langmuir* 2007; **23**: 6205.
[14] Mendoza SM, Arfaoui I, Zanarini S, Paolucci F, Rudolf P. *Langmuir* 2007; **23**: 582.
[15] Petrovykh DY, Kimura-Suda H, Opdahl A, Richter LJ, Tarlov MJ, Whitman LJ. *Langmuir* 2006; **22**: 2578.
[16] Li Y, Huang J, McIver RI Jr, Henninger JC. *J. Am. Chem. Soc.* 1992; **114**: 2428.
[17] Tarlov MJ, Newman JG. *Langmuir* 1992; **8**: 1398.
[18] Frisbie CD, Martin JR, Duff RR, Wrighton MS. *J. Am. Chem. Soc.* 1992; **114**: 7142.
[19] Houssiau L, Bertrand P. *Appl. Surf. Sci.* 2001; **175–176**: 351.
[20] Cyganic P, Vandeweert E, Postawa Z, Bastiaansen J, Vervaecke F, Lievens P, Silverans RE, Winograd N. *J. Phys. Chem. B* 2005; **109**: 5085.
[21] Schröder M, Sohn S, Arlinghaus HF. *Appl. Surf. Sci.* 2004; **231–232**: 164.
[22] Arezki B, Delcorte A, Bertrand P. *Appl. Surf. Sci.* 2004; **231–232**: 122.
[23] Houssiau L, Bertrand P. *Appl. Surf. Sci.* 2001; **175–176**: 399.
[24] Wong SCC, Lockyer NP, Vickerman JC. *Surf. Interface Anal.* 2005; **37**: 721.
[25] Vickerman JC (ed). *Surface Analysis: The Principal Techniques*. Wiley: Chichester, 1997.
[26] Laiho T, Lukkari J, Meretoja M, Laajalehto K, Kankare J, Leiro JA. *Surf. Sci.* 2005; **584**: 83.
[27] Chenakin SP, Heinz B, Morgner H. *Surf. Sci.* 1998; **397**: 84.
[28] Nuzzo RG, Dubois LH, Allara DL. *J. Am. Chem. Soc.* 1990; **112**: 558.
[29] Schoenfisch MH, Pemberton JE. *J. Am Chem. Soc.* 1998; **120**: 4502.
[30] Zharnikov M, Frey S, Heister K, Grunze M. *Langmuir* 2000; **16**: 2697.
[31] Ferral A, Patrito EM, Paredes-Olivera P. *J. Phys. Chem. B* 2006; **110**: 17050.
[32] Vollmer S, Witte G, Wöll C. *Langmuir* 2001; **17**: 7560.
[33] Toulhoat H, Raybaud P, Kasztelan S, Kresse G, Hafner J. *Catal. Today* 1999; **50**: 629.
[34] Sohn S, Schröder M, Lipinsky D, Arlinghaus HF. *Surf. Interface Anal.* 2004; **36**: 1222.
[35] Takakuwa-Hongo C, Tomita M. *Surf. Interface Anal.* 1997; **25**: 966.
[36] Dederichs F, Petukhova A, Daum W. *J. Phys. Chem. B* 2001; **105**: 5210.

